ARTICLE
Journal of Cellular Biochemistry 116:1993–2007 (2015)

Journal of Cellular Biochemistry

The Critical Role of Dynamin-Related Protein 1 in Hypoxia-Induced Pulmonary Vascular Angiogenesis

Tingting Shen,[1] Na Wang,[1] Xiufeng Yu,[1] Jiucheng Shi, Qian Li, Chen Zhang,[1] Li Fu,[1] Shuang Wang,[2] Yan Xing,[3] Xiaodong Zheng,[4] Lei Yu,[1] and Daling Zhu[1,2]*

[1]*Department of Biopharmaceutical Sciences, College of Pharmacy, Harbin Medical University (Daqing), Daqing, China*

[2]*Biopharmaceutical Key Laboratory of Heilongjiang Province, Harbin Medical University, Harbin, China*

[3]*Department of Pharmacology, College of Basic Medicine, Harbin Medical University, Daqing, China*

[4]*Department of Pathophysiology, College of Basic Medicine, Harbin Medical University, Daqing, China*

ABSTRACT

Pulmonary arterial hypertension (PAH) is a lethal disease characterized by pulmonary vascular obstruction due in part to excessive pulmonary artery endothelial cells (PAECs) migration and proliferation. The mitochondrial fission protein dynamin-related protein-1 (DRP1) has important influence on pulmonary vascular remodeling. However, whether DRP1 participates in the development and progression of pulmonary vascular angiogenesis has not been reported previously. To test the hypothesis that DRP1 promotes the angiogenesis via promoting the proliferation, stimulating migration, and inhibiting the apoptosis of PAECs in mitochondrial Ca^{2+}-dependent manner, we performed following studies. Using hemodynamic analysis and morphometric assay, we found that DRP1 mediated the elevation of right ventricular systemic pressure (RVSP), right heart hypertrophy, and increase of pulmonary microvessels induced by hypoxia. DRP1 inhibition reversed tube network formation in vitro stimulated by hypoxia. The mitochondrial Ca^{2+} inhibited by hypoxia was recovered by DRP1 silencing. Moreover, pulmonary vascular angiogenesis promoted by DRP1 was reversed by the specific mitochondrial Ca^{2+} uniporter inhibitor Ru360. In addition, DRP1 promoted the proliferation and migration of PAECs in mitochondrial Ca^{2+}-dependent manner. Besides, DRP1 decreased mitochondrial membrane potential, reduced the DNA fragmentation, and inhibited the caspase-3 activation, which were all aggravated by Ru360. Therefore, these results indicate that the mitochondrial fission machinery promotes migration, facilitates proliferation, and prevents from apoptosis via mitochondrial Ca^{2+}-dependent pathway in endothelial cells leading to pulmonary angiogenesis. J. Cell. Biochem. 116: 1993–2007, 2015.

KEY WORDS: MITOCHONDRIAL FISSION; HYPOXIA; ANGIOGENESIS; MITOCHONDRIAL CALCIUM

Pulmonaryartery hypertension (PAH) is characterized by pulmonary vasoconstriction, remodeling of small pulmonary arteries that leads to increased mean pulmonary arterial pressure, and ultimately to right heart failure and death [Galie et al., 2013]. Studies

Abbreviations: DRP1, dynamin-related protein-1; ER, endoplasmic reticulum; MCU, mitochondrial Ca^{2+} uniporter; MPT, mitochondrial permeability transition; PA, pulmonary artery; PAECs, pulmonary artery endothelial cells; PAH, pulmonary arterial hypertension; PASMCs, pulmonary arterial smooth muscle cells; PI, propidium iodide; PVR, pulmonary vascular remodeling; RVH, right ventricular hypertrophy; RVSP, right ventricular systemic pressure.

Grant sponsor: Key Research Plan of National Natural Science Foundation of China; Grant number: 91339107; Grant sponsor: National Natural Science Foundation of China; Grant number: 81270113; Grant sponsor: Specific Science Foundation for Ph D Training Program of Ministry of Education of China; Grant number: 20112307110022; Grant sponsor: Key Research Plan of Heilongjiang Province of China; Grant number: GC10C206; Grant sponsor: Key Research Plan of Daqing of China; Grant number: SGG2011-05; Grant sponsor: Science and Technique Foundation of Daqing of China; Grant number: DQGX2011KJ002; Grant sponsor: Doctor discipline Foundation of Ministry of Education of China; Grant number: 20112307110022; Grant sponsor: Novel Foundation of Heilongjiang Province of China; Grant number: YJSCX2014-12HYD.

*Correspondence to: Daling Zhu, M.D Ph.D, Department of Biopharmaceutical Sciences, College of Pharmacy, Harbin Medical University (Daqing), Xinyang Road, Daqing, Heilongjiang 163319 P. R. China.
E-mail: dalingz@yahoo.com

Manuscript Received: 22 January 2015; Manuscript Accepted: 3 March 2015

Accepted manuscript online in Wiley Online Library (wileyonlinelibrary.com): 9 March 2015

DOI 10.1002/jcb.25154 • © 2015 Wiley Periodicals, Inc.

by Ma et al. [2011] reveal that dysfunctional angiogenesis is associated with this disastrous disease. Hypoxia induced vascular generation, a common complication of chronic hypoxic lung diseases in the adult pulmonary circulation, is regarded as a potential beneficial adaptation [Howell et al., 2003]. Besides, the new growing arterioles or capillaries increase the oxygen consume and blood perfusion, exacerbating the progression of PAH [Ma et al., 2012]. However, the molecular mechanism under the process of angiogenesis in PAH is rarely known.

Rigorous control over endothelial cells (ECs) migration is necessary in adult angiogenesis [Graupera et al. 2008] and the progress of the embryonic vascular system into a highly organized network [Birdsey et al., 2012]. Meanwhile, angiogenesis was induced by proliferation of pulmonary arterial endothelial cells (PAECs) [Ma et al., 2011]. Moreover, apoptosis-resistance phenotype was observed in the process of angiogenesis in the human umbilical vein endothelial cell [Yang et al., 2014] and mesenchymal stem cells [Legha and Novins, 2012]. It is critical to find some molecules acting the migration, proliferation, and apoptosis of PAECs during angiogenesis.

Mitochondria exist in a dynamic interconnecting network consisting of individual organelles that continuously join (fusion) and fragment (fission). The molecular machinery that mediates this mitochondria fission and fusion is necessary to maintain mitochondrial integrity and intersect apoptosis pathways [Suen et al., 2008]. Dynamin-related protein-1 (DRP1) is a mitochondrial outer membrane protein, mediating mitochondrial fission, and controlling mitochondrial morphology [Otsuga et al., 1998; Westermann, 2010]. The inhibition of DRP1 activation prevents mitochondrial fission and reduces the proliferation of pulmonary arterial smooth muscle cells (PASMCs) during pulmonary vascular remodeling [Marsboom et al., 2012]. However, whether DRP1 participates in the angiogenesis remains elusive.

The regulation of mitochondrial Ca^{2+} ($[Ca^{2+}]_m$) has been confirmed as one significant event and mitochondrial function might suit to various conditions of the living cell [Pivovarova and Andrews, 2010]. Mitochondrial Ca^{2+} loading, originating from Ca^{2+} release from the endoplasmic reticulum (ER) leads to mitochondrial permeability transition (MPT), and depolarization, which is followed by the release of proapoptotic factors activating the effector caspases and triggering apoptotic cell death [Orrenius et al., 2003]. The spatiotemporal properties of mitochondrial Ca^{2+} responses has been reported to be controlled by mitochondrial fission in Hela cells [Szabadkai et al., 2004], indicating that DRP1 may participate in the $[Ca^{2+}]_m$ dependent apoptosis, even migration, and proliferation in vascular cells.

To address these issues we performed the studies in which we combined morphological dynamics and Ca^{2+} imaging to investigate the effect of forced mitochondria to assess overall changes of mitochondrial Ca^{2+} and apoptotic signaling. Our results showed that DRP1 participated in pulmonary arterial angiogenesis through promoting the migration, stimulating the proliferation, and inhibiting the apoptosis of PAECs via mitochondrial Ca^{2+}.

MATERIALS AND METHODS

ANIMALS AND TREATMENTS

Adult male C57BL6/J wild type mice (average weight of 25 g) from the Harbin Medical University Experimental Animal Center were randomly assigned to control or hypoxia groups, as described previously [Zhu et al., 2003]. Mice upon hypoxia were treated with vehicle control and Mdivi-1 (Sigma, M0199, 50 mg/kg, i.p.) according to earlier reports [Chen et al., 2012; Brooks et al., 2009]. All animal experiments complied with the guidelines of the National Institutes of Health (NIH) for the Care and Use of Laboratory Animals, and were approved by the Harbin Medical University Ethical Committee of Laboratory Animals. All surgical procedures were performed under sodium pentobarbital anesthesia.

HEMODYNAMIC ANALYSIS AND VENTRICULAR WEIGHT MEASUREMENT

At the end of the treatment protocol, the animals were anesthetized with intraperitoneally injected with pentobarbital. They were artificially ventilated with 10 ml/kg body weight and a frequency of 60 s^{-1} (SAR830A/P, IITC) after tracheostomy. Inspiratory oxygen (FIO_2) was set at 0.5, and a positive end-expiratory pressure of 1.5 cm H_2O was used throughout. Anesthesia was maintained by inhalation of isoflurane. The left carotid artery was cannulated for systemic arterial pressure (SAP) monitoring, and a Millar (Millar Instruments Inc, Houston, Tex) catheter was inserted through the right jugular vein for measurement of right ventricular systolic pressure (RVSP) with PowerLab (AD Instruments, Colorado Springs, Colo) monitoring equipment. For ventricular weight measurement, hearts were excised, and atria were removed. The RV free wall was dissected, and each chamber was weighed. The ratio of RV weight to left ventricular (LV) weight plus septum (RV/LV+S) was used as an index of RV hypertrophy. After exsanguination, the lung was fixed for histology in 4% paraformaldehyde.

MORPHOMETRIC ANALYSIS OF THE PA

The left lung tissues were sliced into tissue blocks, and immersed in 4% paraformaldehyde for overnight fixation [Shen et al., 2013]. The right lung tissues were fixed in 4% paraformaldehyde for 6 h, transferred to 10%, 20%, 30% sucrose in 0.1 mol/L phosphate buffer (pH 7.4) for 12 h respectively in order to cryoprotection, and stored at 4°C. Lung tissue was frozen in Tissue-Tek OCT compound (Sakura Finetechnical Co) at −20°C. Then, 7 μm sections were cut using a cryostat. The cryosections were blocked with 10% normal goat serum/PBS for 30 min. CD31 (Santa Cruz, 1: 50) and DRP1 (Santa Cruz, 1: 50) was incubated at 4°C overnight. After washing three times with PBS, sections were incubated with Alexa Fluor 488 conjugated mouse anti- goat antibody (Invitrogen, 1: 100) and Alexa Fluor 546 conjugated goat anti-rabbit antibody (Invitrogen, 1: 100) for 2 h at room temperature and DAPI away from light. Sections were washed three times with PBS and then examined with a microscope (Olympus, Japan), and images were recorded by digital photomicrography (Olympus, Japan).

CELL CULTURE

Calf lungs, from a local slaughter house, used in the study were approved by the Harbin Medical University Ethical Committee of Laboratory Animals. Primary cultured PAECs were prepared from pulmonary arteries isolated from calf lungs. The arteries were slit open and gently scratched along the intimal surface with a surgical blade. The purity and identity of PAECs were confirmed by positive

immunofluorescence staining using antibodies to CD31 (Santa Cruz). Cells were cultured in 20% fetal bovine serum (FBS)-DMEM and in a 37°C, 5% CO_2 humidified incubator. Before each experiment, the cells were incubated in DMEM without serum for 24 h. Cells in hypoxic culture were incubated in a Tri-Gas Incubator (Heal Force, Shanghai, China) with a gas mixture containing 92%N_2–5% CO_2–3% O_2 for 24h.

SIRNA DESIGN AND TRANSFECTIONS

To silence the expression of DRP1 protein, PAECs were transfected with small interfering RNA, which was designed, and synthesized by GenePharma. Non-targeted control siRNA (siNC) was used as negative control. The sense sequence of siRNA against DRP1 and non-targeted control sequence were listed below with accession numbers: DNM1 (NM_001076820.1): 5′-GGGACAUGCUUAUGCA-GUUTT-3′; siNC control: 5′-UUCUCCGAACGUGUCACGUTT-3′. Briefly, the PAECs at 50%–70% confluence were used, 1.5 μg siRNA, and 7.5 μl X-treme Gene siRNA Transfection Reagent were separately diluted in 100 μl serum-free Opti-MEM-1 medium for 5 min, after mixed together, and incubated at room temperature for another 20 min, the mixture (siRNA/ Transfection Reagent) was added directly onto the cells. Cells were quiescenced for 24 h and used as required.

IMAGE ANALYSIS OF MITOCHONDRIAL MORPHOLOGY AND MITOCHONDRIAL CALCIUM DETECTION

To quantify mitochondrial fragmentation count (MFC), PAECs were transfected with mitochondrial-targeted, photo activatable green fluorescent protein (mito-PA-GFP). The extent of mitochondrial networking is reflected in the diffusion of the photoactivated mitochondrial GFP away from the site of photo activation, as measured after 17.6 s using NA1.4 inverted Leica DMI6000 microscope (Leica, Heidelberg, Germany), images were visualized by Hamamatsu ORCA-R2 camera (Hamamatsu, Japan) and recorded by LAS AF software (Leica, Heidelberg, Germany).

The $[Ca^{2+}]_m$ (mitochondrial Ca^{2+} concentration) was estimated by loading the PAECs with 4 μM Rhod-2 acetoxymethyl ester, which is compartmentalized into the mitochondria [Hajnoczky et al., 1995]. The Rhod-2 fluorescence was measured using NA1.4 inverted Leica DMI6000 microscope (Leica, Heidelberg, Germany).

TUBE FORMATION ASSAY

Ninety-six-well culture plates (Costar, Corning) were coated with growth factor-reduced Matrigel (BD Biosciences) in a total volume of 30 μl and allowed to solidify for 30 min at 37°C. PAECs were trypsnized and resuspended at 5×10^4 cells/ml and 200 μl of this cell suspension were added into each well. PAECs were administrated under 3% oxygen exposure for 24 h. Vehicle (deoxygenated water) or Ru360 (Santa Cruz) in 10 μM for 30 min were added to the appropriate well. Tube formation was observed under an inverted microscope (Nikon, Japan). Tube length was measured using Image Pro Plus 6.0.

MIGRATION ASSAYS

For scratch-wounding cell migration assay, the confluent PAECs cultured in six-well plates were wounded by pipette tips, given rise to one acellular 1 mm wide lane per well, and the ablate cells were washed out by PBS. PAECs were administrated under 3% oxygen exposure for 24 h. After that, cells were treated with vehicle (deoxygenated water) or Ru360 in 10 μM for 30 min with 5% FBS DMEM. Wounded areas were photographed at zero time. After 6 h, 24 h of incubation, photos were taken from the same areas as those recorded at zero time.

For modified Boyden chamber migration assays, cells were subcultured once, before seeding into the apical (upper) chamber of the transwells. The lower chamber contained the experimental reagents in 10% FBS-DMEM, migration was measured using a modified Boyden chamber with 8 μm-pore polycarbonate filter. Briefly, 8×10^4 PAECs were suspended in DMEM without FBS in the upper chamber of a 24-well Boyden chamber apparatus with serum stimuli in the lower chamber for 24 h, after which the inserts were removed. The non-migrating cells in the upper chamber were then removed with a cotton swab. To stain the cells embedded in the bottom membrane, the inserts were submerged in 4% formaldehyde solution for 10 min followed 0.4% crystal violet in 10% ethanol for 5 min. The number of migrated cells was measured by counting the number of stained nuclei per high-power field in a microscope (Olympus, Japan). Each sample was counted randomly in nine separate locations in the center of the membrane and the endothelial cell migration activity reported as number of cells migrated per field of view. Experiments were performed at least three times in quadruplicate.

MTT ASSAY

PAECs were cultured at a density of 5,000 cells/well in a 96-well culture plate and then treated with Ru360 in DMEM with 5% FBS. At the end of incubation at 37°C, the cells were incubated for 4 h in a medium containing 0.5% 3-[4, 5-dimethylthiazol-2-yl]-2, 5-diphenyl-tetrazolium bromide (MTT), the yellow mitochondrial dye. The amount of blue formazan dye formed from MTT is proportional to the number of survival cells. The reaction was terminated after adding 150 μl DMSO and incubating the cells for 10 min. Absorbance at 540 nm was recorded by an ELISA plate reader.

BROMODEOXYURIDINE INCORPORATION

PAECs were plated in 96-well plates at the density of 5,000 cells/well, and then subject to growth arrest for 24 h before treatments with different agents in 5% FBS DMEM. The cells were administrated under 3% oxygen exposure for 24 h. Vehicle (deoxygenated water) or Ru360 (Santa Cruz) in 10 μM for 30 min were added to the appropriate well. We measured BrdU incorporation according to the Millipore BrdU proliferation assay kit (Catalog No. 2750, Billerica, MA) instructions. Briefly, after treatment, the cells were incubated with 15 μM BrdU labeling solution per well for 24 h at 37°C, and then incubated for 30 min in FixDenat solution at room temperature. Flicking off the FixDenat solution thoroughly, we added anti-BrdU-monoclonal solution 200 μl /well for 1 h at room temperature. Each well was rinsed three times with 200 μl washing solution and incubated for 30 min in 100 μl substrate solution. After adding 100 μl stop solution, the absorbance at 450 nm of the samples was recorded in an ELISA reader.

WESTERN BLOT ANALYSIS

Pulmonary arteries from rats (normoxia, hypoxia, and hypoxia with NDGA) were homogenized in a hand-held micro-tissue grinder in ice-cold storage buffer (Tris 50 mM, pH 7.4, NaCl 150 mM, Triton X-100 1%, EDTA 1 mM, and PMSF 2 mM). The homogenates were sonicated on ice and then centrifuged at 16,099 g for 10 min at 4°C. The supernatants were collected and stored at −80°C until used in Western blot analysis.

PAECs were administrated under 3% oxygen exposure for 24 h. Vehicle (deoxygenated water) or Ru360 (Santa Cruz) in 10 μM for 30 min were added to the appropriate well. After treatments in 6-well culture clusters above, the cells were lysed in a lysis buffer (Tris 50 mM, pH 7.4, NaCl 150 mM, Triton X-100 1%, EDTA 1 mM, and PMSF 2 mM) containing phosphatase inhibitor and incubated for 30 min on ice. The lysates were then sonicated and centrifuged at 16,099 g for 10 min, and the insoluble fraction was discarded. The supernatants were collected and stored at −80°C until used in Western blot analysis.

Protein concentrations were determined by the Bradford assay using bovine serum albumin (BSA) as standard. Pulmonary artery homogenates containing 50 μg of protein and cells protein samples containing 20 μg of protein were separated by SDS–PAGE as previously described. After electrophoresis, proteins were transferred to nitrocellulose sheets. These membranes were blocked in 5% milk and incubated with DRP1 (Santa Cruz, sc-32898, 1:400), PCNA (Santa Cruz, sc-25280, 1:1000), cyclin A (Santa Cruz, sc-596, 1:500), cyclin B1 (Cell Signal, Catalog No. 4138, 1:400), β-actin (Santa Cruz, sc-47778, 1:2000), and secondary antibodies as described. These proteins were visualized with enhanced chemiluminescence reagents (SuperSignal, Pierce).

RELATIVE MRNA QUANTIFICATION BY REAL-TIME POLYMERASE CHAIN REACTION

Total RNA was extracted from cultured PAECs using the Trizol reagent according to the manufacturer's instructions and detected by ultraviolet spectrophotometry. Extracted total RNAs were reverse-transcribed according to the Superscript first-strand cDNA synthesis kit (Invitrogen). cDNA samples were amplified in a DNA thermal cycler (Thermo Scientific, Waltham, MD). The gene-specific primers were designed from coding regions and the nucleotide sequences of primers were as follows: DRP1 (GenBank accession no NM_001076820.1), sense: 5′ -AGTACCTGTTCTGGCTAATGG-3′, anti-sense: 5′ -TCACTTTCGTGCGCTCGTAG-3′, 109 bp) were designed from sequences of the coding regions to that from GenBankTM database. Real-time polymerase chain reaction (PCR) was used for relative quantification of the DRP1 mRNA. The reactions were performed in an ABI 7700 Sequence Detection System (Applied Biosystems, Foster City, Calif).

CELL CYCLE AND DNA ANALYSIS

The Cycle TEST™ PLUS DNA Reagent Kit obtained from BD Biosciences (Bedford, MA) was used for examining whether the cell cycle was regulated by DRP1. PAECs were treated in groups as indicated and then harvested with trypsin and fixed using 70% ethanol. The ethanol was removed, and the cells were incubated in 200 μl PBS. The cells were stained according to manufacturer's protocol. DNA fluorescence was measured and flow cytometry was performed using BD FACS Calibur Flow Cytometer (Bedford, MA). For each sample, 2×10^5 events were accumulated in a histogram. The proportions of cells in the different phases of the cell cycle were calculated from each histogram.

MEASUREMENT OF CASPASE ACTIVITY

PAECs were administrated under 3% oxygen exposure for 24 h. Vehicle or Ru360 (Santa Cruz) in 10 μM for 30 min were added to the appropriate well. Caspase-3 activity was determined using a caspase-3 activity assay kit (Sigma). The cells were lysed in caspase-3 sample lysis buffer provided in the kit. The homogenates were centrifuged at 10,000 g, and the supernatant was collected for protein estimation (BCA method) and for caspase-3 assay. Cleavages of Ac-DEVD-pNA (acetyl-Asp-Glu-Val-Aspp-nitroanilide), caspase-3 substrate were examined for caspase-3 activity as the protocols provided in the kit. Lysates were incubated at 37°C for 2 h. Thereafter, the sample was measured in an automatic microplate reader (SpectraMax M5) at excitation 400 nm and emission 505 nm. The specific caspase-3 activity was normalized to the total protein and then expressed as fold of caspase-3 activity.

FLOW CYTOMETRY

Annexin V-PE, 7-AAD kit was used to measure the percentage of apoptosis in accordance with the manufacturer's protocols (BD Biosciences). PAECs were administrated under 3% oxygen exposure for 24 h. Vehicle or Ru360 (Santa Cruz) in 10 μM for 30 min were added to the appropriate well. Briefly, after treatments, cells (1×10^5) were collected and resuspended in 100 ml of binding buffer containing 5 ml annexin V-PE and 5 ml 7-AAD, then incubated for 15 min in the dark at room temperature, and the percentage of apoptotic cells was immediately assessed using a flow cytometer.

MITOCHONDRIAL DEPOLARIZATION ASSAY

PAECs were administrated under 3% oxygen exposure for 24 h. Vehicle or Ru360 in 10 μM for 30 min were added to the appropriate well. We monitored the mitochondrial membrane potential by determining the relative amounts or dual emissions from both monomers (green) and aggregates (red) of mitochondrial 5,5′,6,6′-tetrachloro-1,1′,3,3′-tetraethyl benzimidazol carbocyanine iodide (JC-1) using an Olympus fluorescent microscope under Argon-ion 488 nm laser excitation. Images obtained by a fluorescent microscope were analyzed for green and red fluorescence. Mitochondrial depolarization was expressed by an increase in the intensity ratio of green/red fluorescence.

TUNEL

Labeling 3′-end of fragmented DNA of apoptotic cells by TdTUTP nick end labeling (TUNEL) method was performed in PAECs. The cells cultured in a 6-well plate were treated as mentioned above, administrated under 3% oxygen exposure for 24 h. Vehicle or Ru360 in 10 μM for 30 min were added to the appropriate well then fixed with 4% paraformaldehyde phosphate buffer saline, rinsed with PBS, and then permeabilized by 0.1% TritonX-100 for 2 min on ice

followed by TUNEL for 1 h at 37°C. The FITC-labeled TUNEL-positive cells were imaged under a fluorescent microscopy at 488 nm excitation and 530 nm emission. The cells with green fluorescence were defined as apoptotic cells.

STATISTICAL ANALYSIS

The composite data are expressed as means ± SEM. Statistical analysis was performed with Student's *t*-test or one-way ANOVA followed by Dunnett's test where appropriate. $P < 0.05$ was considered statistically significant.

RESULTS

DRP1 INHIBITION PREVENTED INCREASE OF MICROVESSELS INDUCED BY HYPOXIA IN VIVO

To determine whether DRP1 is involved in the pathogenesis of PAH, we tested DRP1 inhibitor Mdivi-1 in experimental mouse model of PAH. Hypoxia significantly elevated right ventricular systemic pressure (RVSP) compared with sham-control group (Fig. 1A and B). Consistently, the RV/LV+S ratio was significantly increased in the hypoxia group compared with the sham-control mice (Fig. 1C). However, DRP1 inhibitor Mdivi-1 significantly reversed the augmentation of RVSP and RV/LV+S ratio induced by hypoxia. We found that Mdivi-1 inhibited the proportion of DRP1 positive cells induced by hypoxia in the pulmonary vessels (Fig. 1D and E).

To demonstrate the role of DRP1 in the arterioles increase, we detected the density of microvessels in hypoxia mouse model. Hypoxic exposure increased the percentage of $CD31^+$ cells compared to control subjects in vessels of which the diameters were 50–150 μm (Fig. 1D and F, the data of vessels of which the diameters were 20–50 μm, and <20 μm were not shown here). After treatment with mdivi-1 these hypoxia-induced increases were significantly reduced. These results implicate a role of DRP1 in hypoxia-induced angiogenesis associated with the development of experimental pulmonary hypertension.

DRP1 COULD BE INDUCED BY HYPOXIA AND MEDIATED TUBE FORMATION IN VITRO

To test whether hypoxia affected the expression of DRP1, we administrated the PAECs under 3% oxygen exposure. We found that hypoxia induced a time dependent increase of the DRP1 expression in both transcriptional levels and posttranscriptional levels, with peaks 12–24 h after hypoxia exposure (Fig. 2A and B).

DRP1 mediated mitochondrial fission and controlled mitochondrial morphology [Otsuga et al., 1998; Westermann, 2010]. Hypoxia exposure induced the mitochondria more fragmented, while after we knocked down the gene of DRP1 (the efficiency of transfection was shown in Fig. 2C), the morphology of mitochondria became continuously joined (Fig. 2D).

To determine whether DRP1 mediated angiogenesis ex vivo, we performed PAEC tube formation assay. Our results showed that hypoxia stimulated PAEC tube formation compared with control in normoxia, while silencing the DRP1 gene significantly reduced the tube formation induced by hypoxia (Fig. 2E).

PAEC MIGRATION WAS REGULATED BY DRP1

To elucidate whether DRP1 was involved in PAEC migration, we knocked down DRP1 with siRNA. In the scratch-wound assay, hypoxia induced migration was significantly inhibited in DRP1 depleted PAECs (Fig. 2F). In addition, we examined the effects of DRP1 during PAEC migration in a modified Boyden chamber. Accordingly, PAEC migration was abolished by silencing DRP1 (Fig. 2G). These results indicate that DRP1 regulates the migration of PAECs under hypoxic conditions.

THE PROLIFERATION AND CELL CYCLE DISTRIBUTION OF PAECS WERE MEDIATED BY DRP1

To determine the effect of DRP1 on PAEC proliferation, cell viability was examined by the MTT assay. Silencing the gene of DRP1, cell viability induced by hypoxia was decreased (Fig. 3A). We observed similar phenotypes in cell proliferation by using BrdU incorporation assay (Fig. 3B) and detecting the expression of the proliferating cell nuclear antigen (PCNA) in PAECs (Fig. 3C). These results indicate that the DRP1 regulates the proliferation of PAECs under hypoxia.

Since cyclin A and cyclin B1 play important roles in both the S and G_2/M phases [Paterlini et al., 1993], we analyzed the posttranslational levels of cyclin A and cyclin B1 in PAECs. A significant reduction in the expression of cyclin A and cyclin B1 was observed after knocking down the gene of DRP1 (Fig. 3C). Hypoxia induced cell proliferation was demonstrated by an increased percentage of cells entering S-phase. The amount of S-phase cells was significantly decreased and the percentage of G_0/G_1-phase cells was increased in DRP1 siRNA-treated hypoxic PAECs. Compared with cells treated with the control siRNA, the percentage of cells in S phase was decreased by 5.02%, accompanied with a concomitant increase of cells in the G_0/G_1 phase from 64.46% to 71.87% (Fig. 3D). These data show that the DRP1 is involved in the cell cycle control of PAECs.

THE INHIBITION OF DRP1 CAUSED MITOCHONDRIAL-DEPENDENT APOPTOSIS

The cell fluorescence changed from red (high $\triangle\psi_m$) to green (low $\triangle\psi_m$) when the mitochondrial membrane potential decreased [Ma et al., 2010]. We used the JC-1 probe to detect the change of mitochondrial membrane potentials and to determine whether the DRP1 pathway was crucial for PAECs survival. Our results revealed that treatment with DRP1 siRNA resulted in an increased ratio of green to red in JC-1-stained PAECs (Fig. 4A).

THE INHIBITION OF DRP1 RESULTED IN DNA FRAGMENTATION AND INDUCED APOPTOSIS

The TUNEL assay refers to terminal transferase (TdT)-based procedures that can detect free DNA ends accompanying chromatin fragmentation, which is a hallmark of apoptotic cells [Gavrieli et al., 1992]. Our results revealed that hypoxia led to a reduction in the number of TUNEL-positive PAECs, and the effect was greatly reversed by knocking down the gene of DRP1 (Fig. 4B).

We then undertook flow cytometer analysis with Annexin V and propidium iodide (PI) staining as another assay for apoptosis. In PAECs, the population of Annexin V-positive cells (apoptotic cells) was decreased under hypoxia exposure. However, siDRP1 treatment increased the

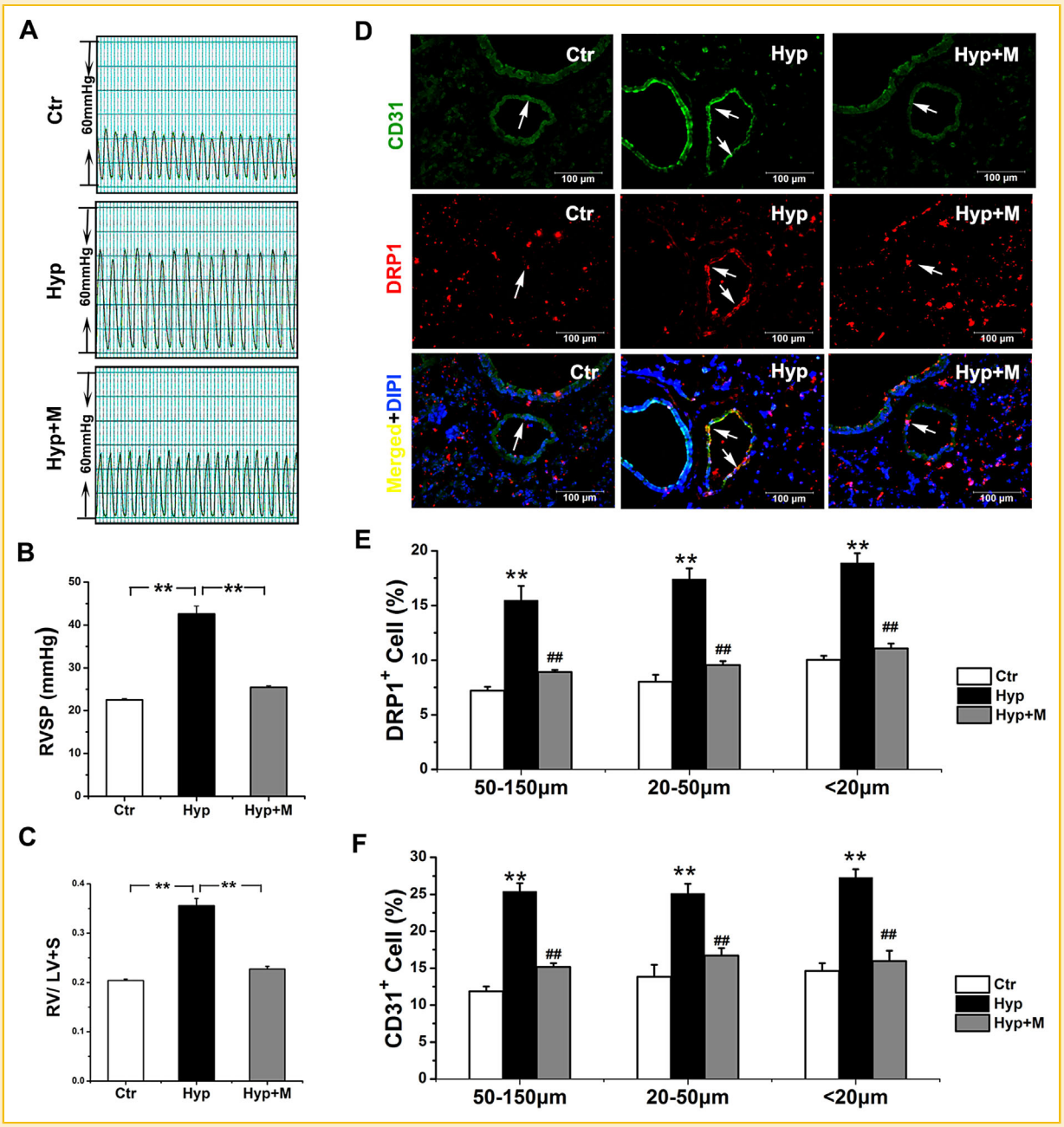

Figure 1. DRP1 inhibition reversed pulmonary vascular angiogenesis. (A), Representative tracing of RVSP. (B), The statistics of RVSP. (C), Ratio of right ventricle to left ventricle plus septum. Hypoxia significantly increased RVSP and aggravated the ratio of right ventricle compared with normoxic mice, which was partially reversed by administration of Mdivi-1 (DRP1 inhibitor, 20 mg/kg body weight). (D) Immunofluorescence of PAs from control, hypoxia, and hypoxia with Mdivi-1 administration mice. Lung sections were stained with (49,69-diamidino-2-phenylindole (DAPI), blue), CD31 (green), DRP1 (red), and Merged (yellow). Quantitative analysis of the intensity of DRP1 (E) and CD31 (F) in vessels of different diameters were shown. Ctr, control; Hyp, hypoxia; M, Mdivi-1. $^{*}P < 0.05$, $^{**}P < 0.01$. n = 5. All values are denoted as mean ± SEM.

proportion of apoptotic cells compared with normoxic or hypoxic cells with siNC treatment (Fig. 4C). Similar results were acquired that the stimulatory roles of DRP1 in caspase-3 activation (Fig. 4D).

MITOCHONDRIAL CA^{2+} LEVEL WAS INDUCED BY DRP1 INHIBITION

Previous reports from Ziviani et al. [2010] suggest that sample fixation alters the mitochondrial morphology. Thus cells were imaged live using the selective mitochondrial dye mitotracker green (Fig. 5A). As expected, we found that knockdown the gene of DRP1 resulted in elongated mitochondria of PAECs (Fig. 2B, 7A), while hypoxia exposure increased mitochondria fragment counts, which was inhibited by siDRP1 (Fig. 5A–B). Oxygen-bridged dinuclear ruthenium amine complex (Ru360), a highly selective inhibitor of mitochondria Ca^{2+} uptake by blocking the mitochondrial Ca^{2+}

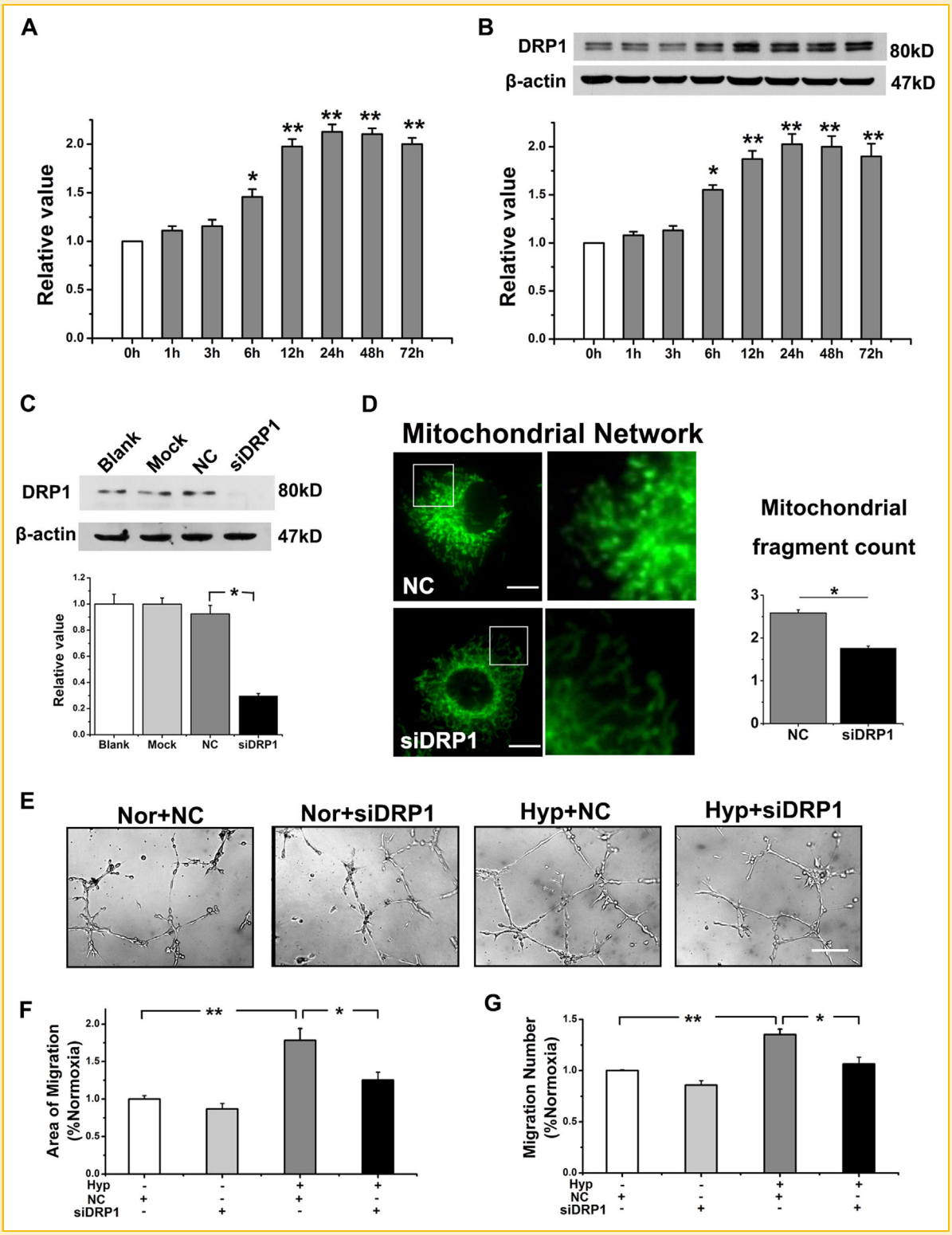

Figure 2. DRP1-mediated tube formation and PAECs migration in vitro. (A) Realtime-PCR of DRP1 exposed to hypoxia. (B) Western blot of DRP1 administrated with hypoxia. (C) The transfection efficiency of DRP1. (D) Mitochondria are less fragmented after silencing the gene of DRP1. Quantification (mitochondrial fragmentation count) reveals a doubling of the number of individual mitochondria in siDRP1 versus control PAECs. Scale bar = 20μm. (E) Knocking down the gene of DRP1 inhibited cell tube formation induced by hypoxia. Scale bars = 50μm. (F), Scratch-wounding cell migration assay. The migration induced by hypoxia was blocked by silencing DRP1. (G), Transwell assays coincident with the results from scratch test. Cells were plated in the upper chamber of the filters. At 24 h after plating, cells that had migrated to the underside of the filters were fixed, and stained with crystal violet. Relative cell migration was determined by the number of migrated cells. Blank, only treating cells with DMEM; Mock, only treating cells with transfection reagent; NC, the negative control sequence. Nor, normoxia; Hyp, hypoxia; NC, negative control. *$P < 0.05$; **$P < 0.01$, n = 5. All of the values are denoted as mean ± SEM.

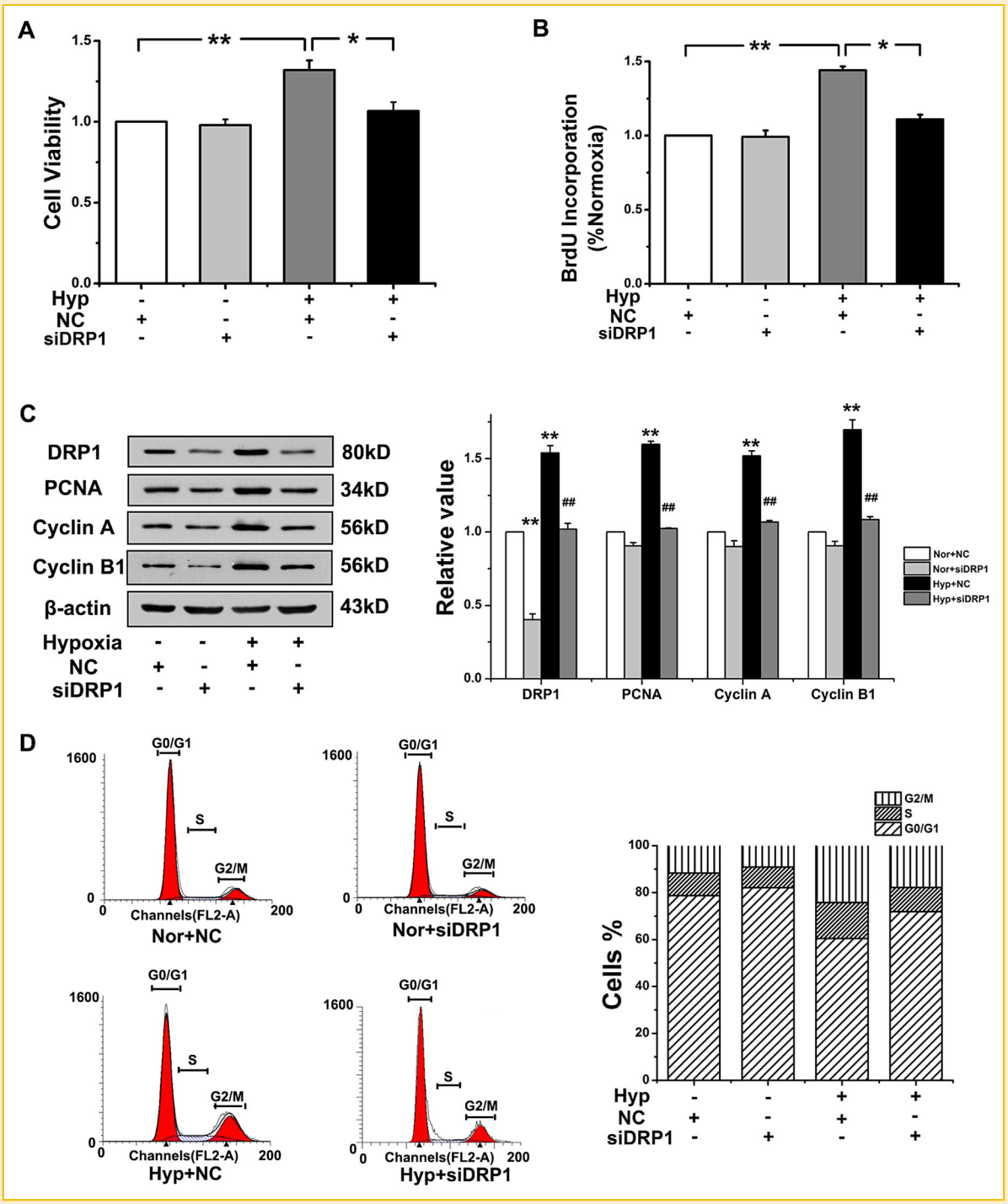

Figure 3. PAECs proliferation and cell cycle distribution induced by hypoxia was inhibited by DRP1 depletion. (A) MTT assay showed that the cell viability in hypoxia-induced PAECs growth. (B) 5-Bromodeoxyuridine (BrdU) incorporation study demonstrated that hypoxia-induced DNA synthesis was blocked by silencing DRP1. $^{*}P < 0.05$, $^{**}P < 0.01$, $n = 6$. (C) The protein expression of PCNA, Cyclin A, and Cyclin B1 were determined after knocking down DRP1. $^{**}P < 0.01$ compared with Normoxia and NC, ## $P < 0.01$ compared with Hypoxia and NC, $n = 3$. (D) The number of cells in each phase of the cell cycle was examined by FACS analysis ($n = 2$). The results showed that inhibiting DRP1 reduced the percentage of cells in S phase accompanied with a concomitant increase of cells at G_0/G_1 phase. Hyp, Hypoxia; si, siDRP1; NC, negative control sequence. All of the values are denoted as mean ± SEM.

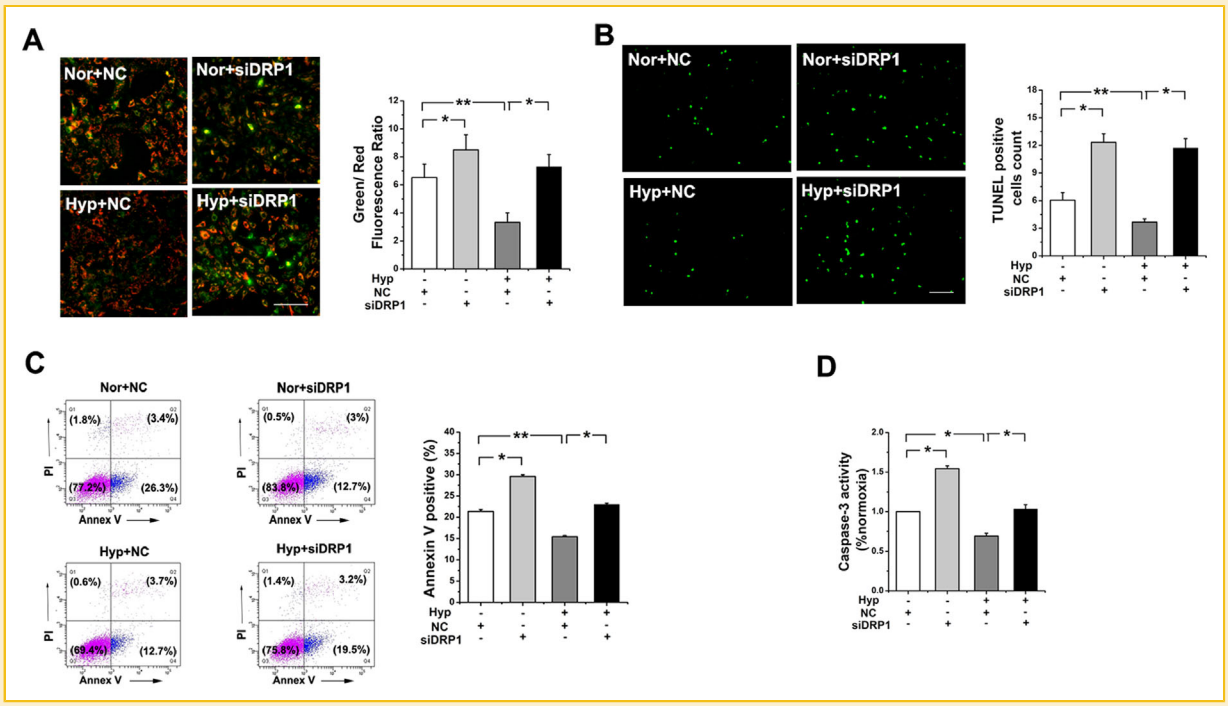

Figure 4. The inhibition of DRP1 caused apoptosis of PAECs. (A) PAECs were stained with JC-1 probe and imaged by the fluorescent microscope and quantitative analysis of the shift of mitochondrial green fluorescence to red fluorescence from six randomly selected fields obtained from each group. We found the loss of mitochondrial membrane potential caused by hypoxia was prevented by siDRP1 ($n = 6$, $^*P < 0.05$). Scale bars = 20 μm. (B) Cells undergoing apoptosis were positively stained with TUNEL reagent and are shown in green. Here are the representative photographs of TUNEL staining in different groups, and quantitative analysis of TUNEL positive cells content among groups ($n = 3$, $^*P < 0.05$). Scale bars = 10 μm. (C) Apoptosis analysis by flow cytometer showed that the reduction of apoptotic cells caused by hypoxia was reversed by DRP1 inhibition ($n = 3$, $^*P < 0.05$). (D) Hypoxia inhibited caspase-3 activation via DRP1 ($n = 6$, $^*P < 0.05$). All values are denoted as mean ± SEM.

uniporter (MCU) was reported to result in the decrease of mitochondrial Ca^{2+} [Kannurpatti and Biswal, 2008]. Our results showed that Ru360 induced PAEC mitochondrial fragmented, which was reversed by silencing DRP1 (Fig. 5A–B). These results demonstrate that DRP1 regulates the mitochondrial fission of PAECs via MCU.

The $[Ca^{2+}]_m$ (mitochondrial Ca^{2+} concentration) was estimated by loading the PAECs with 4 μM Rhod-2 acetoxymethyl ester, which is compartmentalized into the mitochondria [Hajnoczky et al., 1995]. Silencing the gene of DRP1 significantly enhanced the intensity of Rhod-2 fluorescence, suggesting DRP1 inhibited the mitochondrial Ca^{2+}. However, over a period of 30 min, $\triangle F/F_0$ decreased robustly by hypoxia, which was reversed by siDRP1. Hypoxia reduced mitochondrial Ca^{2+} was aggravated by Ru360, which was recovered by siDRP1 (Fig. 5C). These results show that the mitochondrial Ca^{2+} inhibited by hypoxia is mediated by DRP1 in a MCU-dependent manner.

MCU MEDIATED IN THE DRP1 INDUCED FORMATION OF TUBE NETWORKS AND PAEC MIGRATION

Our results showed that Ru360 stimulated PAEC tube formation compared with control under hypoxic condition, while silencing the DRP1 gene significantly reduced the tube formation induced by Ru360 (Fig. 6A). These results demonstrate that DRP1 regulate the migration of PAECs is mitochondrial Ca^{2+}-dependent.

As shown in the scratch-wound assay, the Ru360 induced migration was significantly inhibited in DRP1 depleted PAECs (Fig. 6B). In addition, we examined the effects of DRP1 during PAEC migration induced by serum. Accordingly, PAECs serum response observed in a modified Boyden chamber was significantly induced by ruthenium red, which was recovered by silencing DRP1 (Fig. 6C). These results demonstrate that DRP1 regulates the migration of PAECs via MCU.

The proliferation and cell cycle distribution of PAECs were mediated by DRP1 in a mitochondrial Ca^{2+}-dependent manner

Our results demonstrated that Ru360 promoted cell viability induced by hypoxia, while silencing the DRP1 gene significantly reduced the cell viability induced by Ru360 (Fig. 7A). We observed similar phenotypes in cell proliferation by using BrdU incorporation assay (Fig. 7B) and detecting the expression of the proliferating cell nuclear antigen (PCNA) in PAECs (Fig. 7C). These results indicate that the proliferation of PAECs mediated by DRP1 was mitochondrial Ca^{2+}-dependent.

As detected by flow cytometry, the amount of S-phase cells was significantly increased in Ru360 -treated hypoxic PAECs, which was decreased after treating with the siDRP1 (Fig. 7D). A significant augment in the expression of cyclin A and cyclin B1 induced by hypoxia and Ru360 treatment was observed after knocking down DRP1 (Fig. 7C). These data show that the DRP1 involves in the cell cycle control of PAECs in a mitochondrial Ca^{2+}-dependent manner.

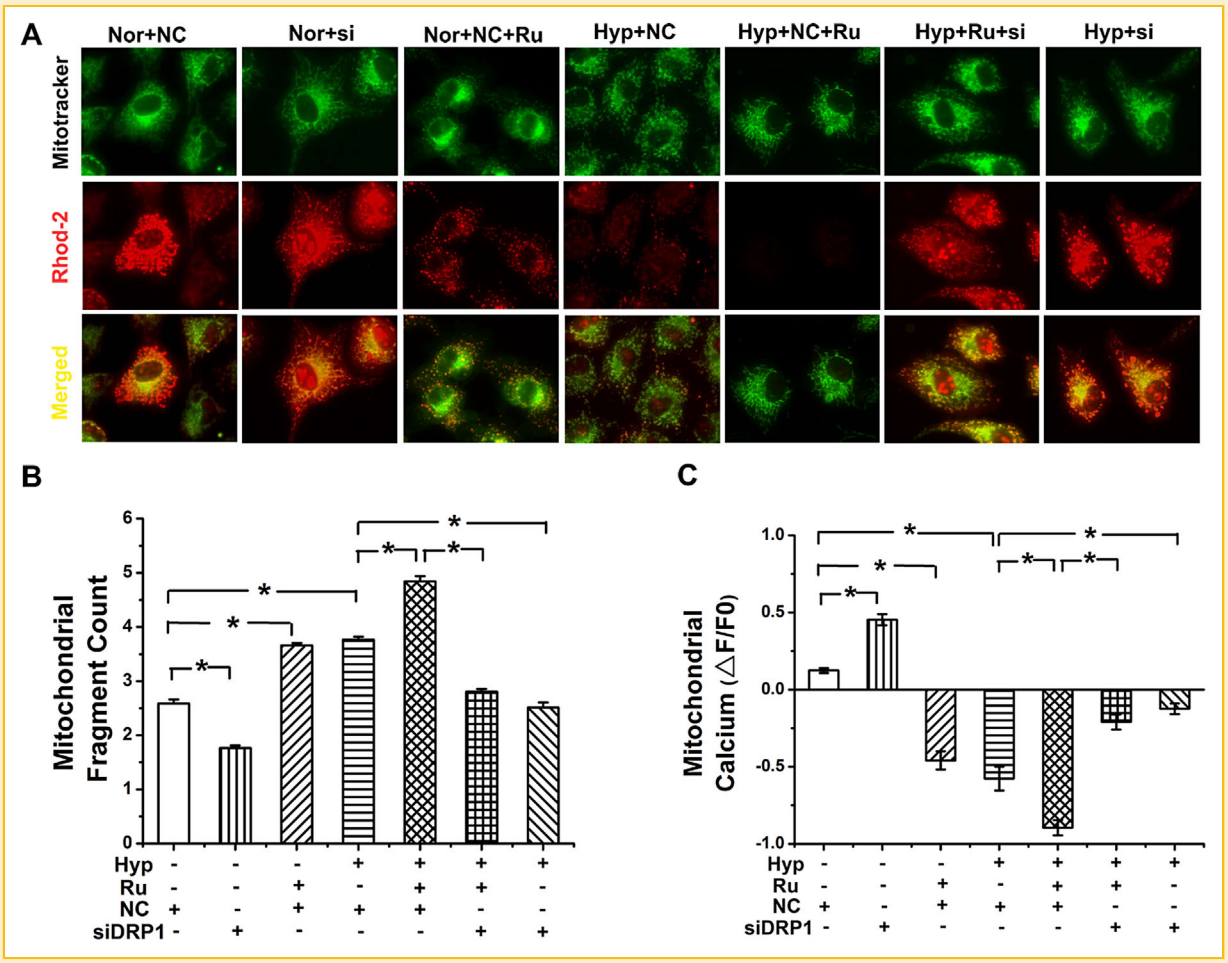

Figure 5. Mitochondrial Ca^{2+} level was induced by DRP1 inhibition. (A) Representative images of PAECs (upper panels) showing hypoxia induced fragmentation of the mitochondrial network was inhibited by siDRP1. Representation of images by mitochondrial specific dye Rhod-2 staining (middle panels) showing Ca^{2+} waves propagating in the whole mitochondrial network. The merged of Mitotracker and Rhod-2 was shown in the lower panels. Quantification of mitochondrial fragmentation count (B) and calculated relative intensity changes (△F/F) of mitochondrial Ca^{2+} (C) were shown. The cells cultured in a petri dish were treated as mentioned above, administrated under 3% oxygen exposure for 24 hours. Vehicle (deoxygenated water) or Ru360 in 10 μM for 30 min were added to the appropriate well. Nor, normoxia; Hyp, hypoxia; NC, negative control; si, siDRP1; Ru, Ru360. n = 6, $^*P < 0.05$. All values are denoted as mean ± SEM.

THE INHIBITION OF DRP1 CAUSED APOPTOSIS WAS MITOCHONDRIAL CA^{2+}-DEPENDENT

We found that the cell viability of PAECs was significantly induced by Ru360 in 10 μM for 30 min (Fig. 8A). According to Figure 8B, the caspase-3 activation inhibited by Ru360 was reversed by knocking down the gene of DRP1. Besides, the population of Annexin V-positive cells (apoptotic cells) was decreased after Ru360 administration; the decreased effect was reversed by siDRP1 treatment (Fig. 8C). Similar results were acquired in TUNEL staining, which showed that the number of TUNEL-positive cells restrained by Ru360 was reversed by silencing the gene of DRP1 (Fig. 8D).

DISCUSSION

In this paper, we provide the first evidence that DRP1 involved in pulmonary vascular angiogenesis. The novel finding of this study is threefold. Firstly, the present study highlights a pivotal role of DRP1 in the pulmonary angiogenesis, simultaneously increased right ventricular systemic pressure, and right ventricular hypertrophy induced by hypoxia. Secondly, we prove that DRP1 mediated tube formation in vitro and decreased the mitochondrial Ca^{2+} accumulation. Thirdly, we find that DRP1 promoted the migration, stimulated the proliferation and inhibited the apoptosis of PAECs in a mitochondrial Ca^{2+}-dependent manner.

It has been reported [Marsboom et al., 2012] that the unbalance of mitochondrial fission and fusion contributes to pulmonary vascular remodeling associated with PAH, and DRP1 is a key regulator in the proliferation of PASMCs. However, our results showed that DRP1 participated in the process of pro-migration, pro-proliferation, and anti-apoptosis of PAECs. The results indicate the novel role of mitochondrial dynamics regulated by DRP1 in pulmonary vascular remodeling. More importantly, alveolar low oxygen results into hypoxic blood contact with the endothelium primarily and then the

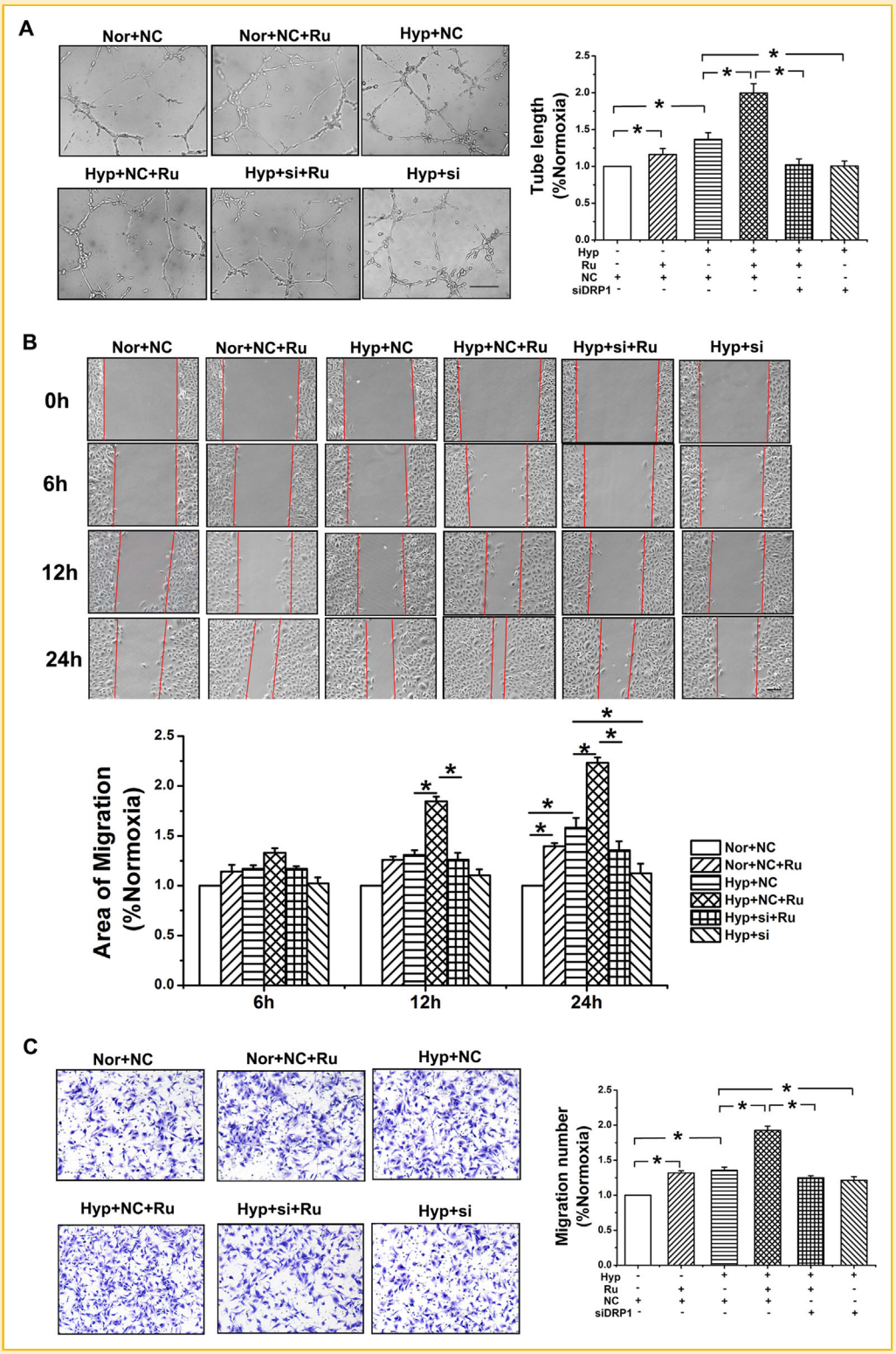

Figure 6. DRP1 advanced tube formation and PAEC migration via MCU. (A) The tube formation of PAECs induced the MCU blocker Ru360 is significantly restrained by siDRP1. (B) The MCU blocker Ru360 induced migration is significantly inhibited in DRP1 depleted PAECs. (C) Transwell assays coincident with the results from scratch test. Cells were plated in the upper chamber of the filters. At 6, 12, 24 h after plating, cells that had migrated to the underside of the filters were fixed and stained with crystal violet. The cells cultured in a 6-well plate were treated as mentioned above, administrated under 3% oxygen exposure for 24 h. Vehicle (deoxygenated water) or Ru360 in 10 μM for 30 min were added to the appropriate well. Relative cell migration was determined by the number of migrated cells. Nor, normoxia; Hyp, hypoxia; NC, negative control; si, siDRP1; Ru, Ru360. $^{*}P < 0.05$; $^{**}P < 0.01$, n = 3. Scale bars are 50 μm. All of the values are denoted as mean ± SEM.

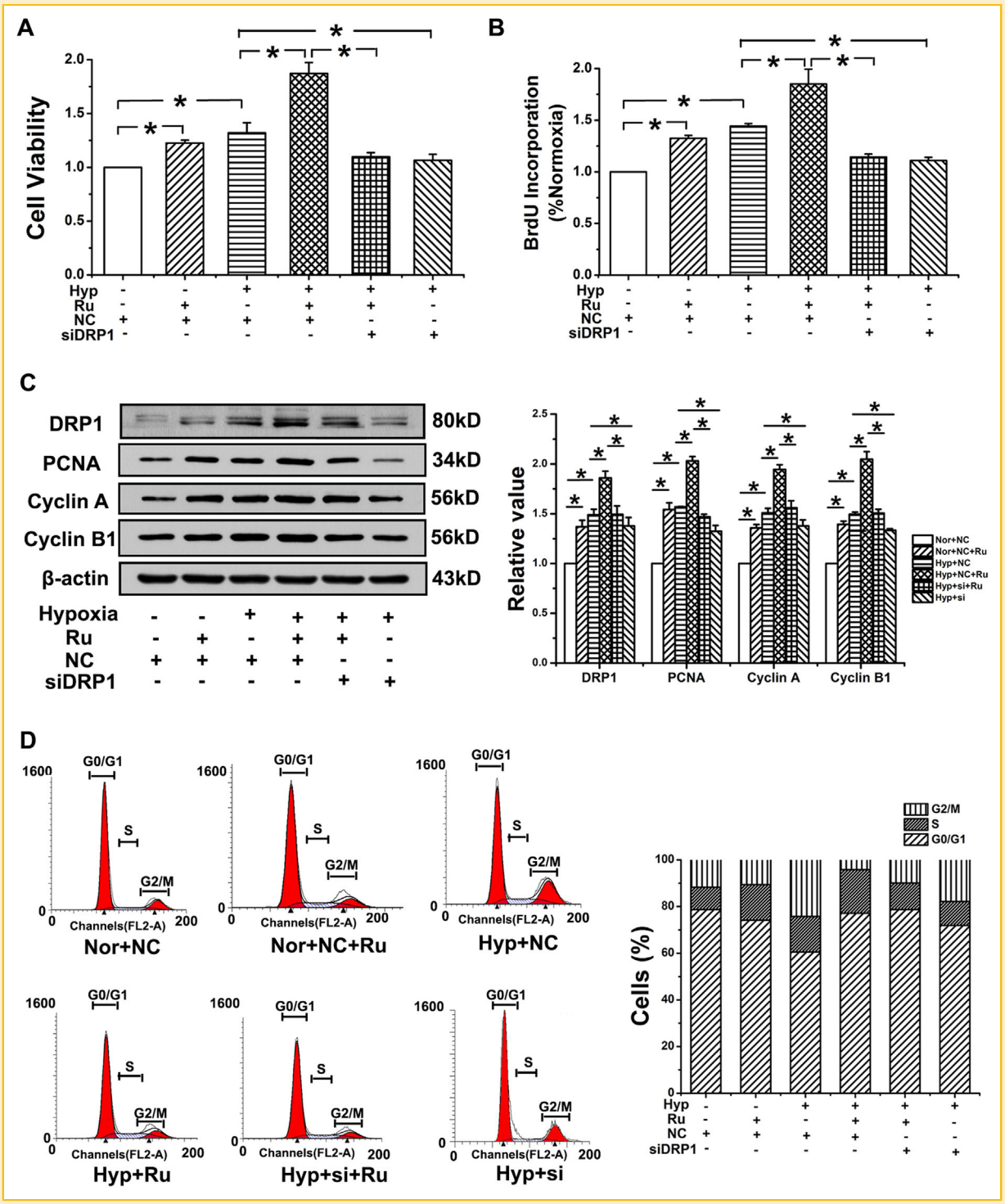

Figure 7. DRP1 mediated PAECs proliferation and cell cycle distribution in a mitochondrial Ca^{2+}-dependent manner. (A) The cell viability measured by MTT assay induced by Ru360 was inhibited by knocking down the gene of DRP1. (B) 5-Bromodeoxyuridine (BrdU) incorporation study demonstrated that hypoxia-induced DNA synthesis was promoted by Ru360, which was restrained by silencing DRP1. (C) The protein expression of PCNA, Cyclin A and Cyclin B1 were determined after knocking down DRP1. *$P < 0.05$, $n = 6$. (D) The number of cells in each phase of the cell cycle was examined by FACS analysis ($n = 2$). The results showed that inhibiting Ru360 increased the percentage of cells in S phase accompanied with a concomitant reduce of cells at G_0/G_1 phase, which was reversed by siRNA of DRP1. PAECs cultured in a 6-well plate were treated as mentioned above, administrated under 3% oxygen exposure for 24 h. Vehicle (deoxygenated water) or Ru360 in 10 μM for 30 min were added to the appropriate well. Hyp, Hypoxia; si, siDRP1; NC, negative control sequence; Ru, Ru360. All of the values are denoted as mean ± SEM.

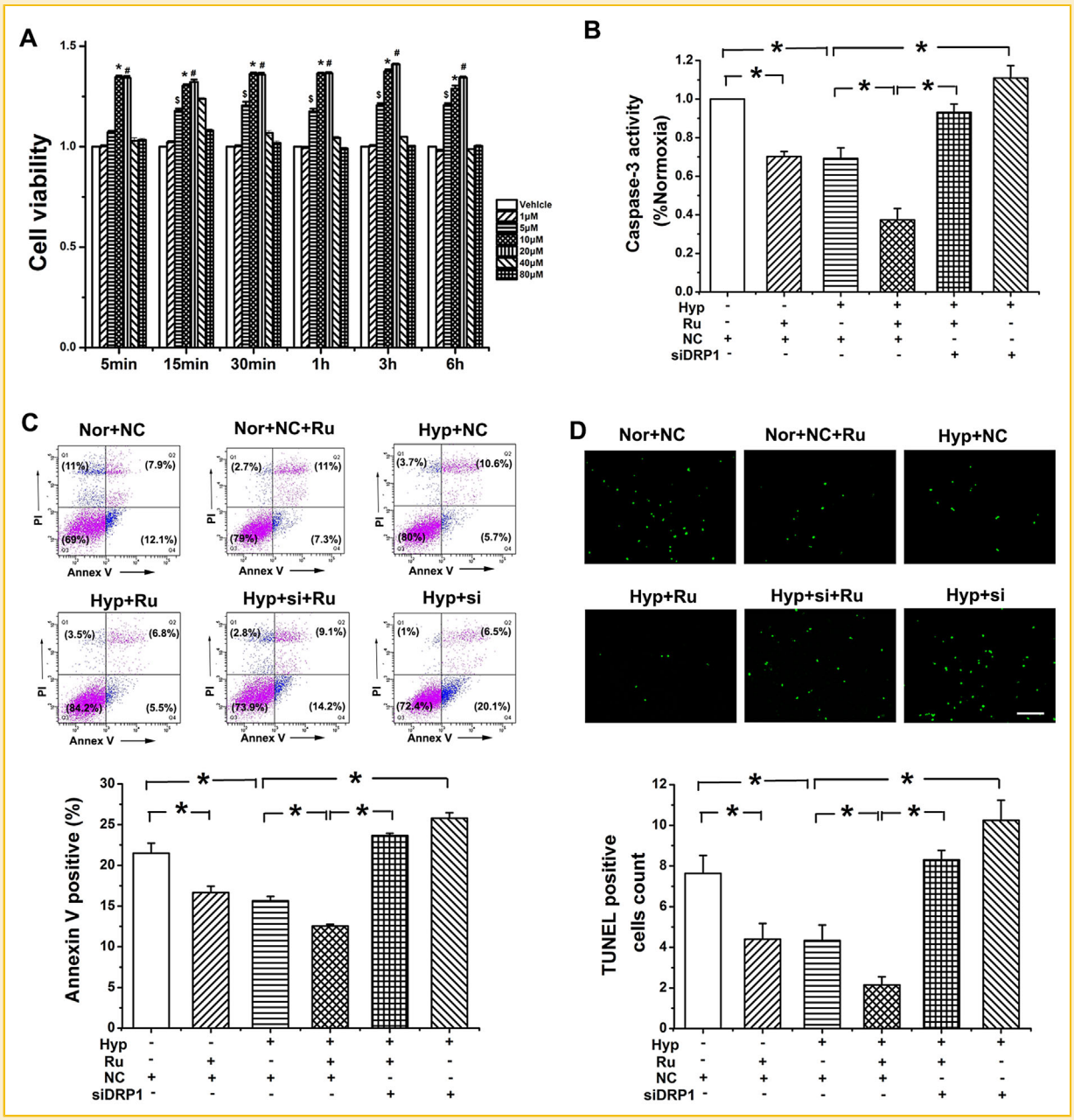

Figure 8. The inhibition of DRP1 caused apoptosis was mitochondrial Ca^{2+}-dependent. (A) MTT assay showed that the cell viability in Ru360 addition (1, 5, 10, 20 μM) for 5 min, 15 min, 30 min, 0.5 h, 1 h, 3 h, and 6 h respectively. (B) Ru360 inhibited caspase-3 activation restrained by hypoxia was reversed by DRP1 inhibition. (C) The DRP1 mediating Ru360-inhibited apoptosis as determined by flow cytometer. (D) Silencing the gene of DRP1 decreased the number of TUNEL-positive cells via the MCU inhibitor in PAECs. PAECs cultured in a 6-well plate were treated as mentioned above, administrated under 3% oxygen exposure for 24 h. Vehicle (deoxygenated water) or Ru360 in 10 μM for 30 min were added to the appropriate well. Hyp, Hypoxia; si, siDRP1; NC, negative control sequence; Ru, Ru360. *$P < 0.05$, n = 6. Scale bars = 20 μm. All values are denoted as mean ± SEM.

media of vessel, leading to the development of pathological progress [Pak et al., 2007]. Thus the effect of DRP1 on PAEC migration, proliferation and apoptosis may act as an onset of the proliferation of PASMCs, further demonstrating the role of mitochondrial dynamics in the fetal disease.

The migration of PAECs is necessary in adult angiogenesis and early stage of vascular development [Jones et al., 2006; Graupera et al., 2008; Birdsey et al., 2012]. Our results firstly report that hypoxia induced migration is significantly restrained in DRP1 depleted PAECs by scratch-wound assay and transwell test (Fig. 3A–B). There are similar results that inhibitor of mitochondrial uncoupling agent or mitochondrial fission protein decreased migration and invasion of breast cancer cell [Zhao et al., 2013] or glioblastoma U251 cells [Wan et al., 2014]. Therefore, our results prove the solid evidences that DRP1 mediated in hypoxia-induced migration of PAECs, resulting to the dysfunctional pulmonary angiogenesis.

Meanwhile, the proliferation of PAECs plays a key role of excessive pulmonary angiogenesis and endothelial dysfunction [Ma et al., 2013]. We prove that DRP1 mediated in the hypoxia induced the cell viability and proliferation in a mitochondrial Ca^{2+} -dependent manner in PAECs. Morphodynamic changes of mitochondria are closely linked to the cell cycle regulators governing the S phase and G2/M phase, including cyclin A and cyclin B1 [Lee et al., 2014]. We find that DRP1 promotes the cell transition from G_0/G_1 phase to S phase and increases the hypoxia induced expression of cyclin A and cyclin B1. Our results indicate that the DRP1 plays a key role of cell cycle regulation in the PAECs via mitochondrial Ca^{2+}.

In addition, the pathologically elevated pulmonary vascular pressure is strongly linked with apoptosis-resistance phenotype of endothelial cells [Courboulin et al., 2011; White et al., 2014], and mitochondrial dynamics especially mitochondrial fission plays a key role in cell apoptosis [Suen et al., 2008]. We find that firstly, the mitochondrial membrane potential augments when administrating the siDRP1 (Fig. 4A). Secondly, the DNA chromatin fragmentation increases after silencing the gene of DRP1 (Fig. 4B). Thirdly, the Annexin V-positive cells indicating apoptotic cells was upregulated after knocking down the gene of DRP1 (Fig. 4C). These evidences suggest that DRP1 inhibits mitochondrial-dependent apoptosis in PAECs. Furthermore, the results on caspase-3 activation which is the early event of mitochondrial apoptosis pathway [Correa et al., 2007] reinforces the previous conclusion. Interestingly, mitochondrial fission stimulated by ceramides is associated with early activation of apoptosis in the cardiomyocyte [Parra et al., 2008] while our results showed that DRP1 inhibition caused mitochondrial-dependent apoptosis of PAECs. The difference of DRP1 in the cell apoptosis between cardiomyocytes and pulmonary vascular cells could be caused by the discrepancy between systemic and pulmonary circulation or the cell specificity.

Our results reveal that mitochondrial Ca^{2+} is involved in the process of cell migration promoted by this mitochondrial fission protein. The Ru360 induced migration is significantly restrained in DRP1 depleted PAECs (Fig. 6B–C). We further demonstrate the relationship between mitochondria and calcium signaling and to our knowledge this is the first report that DRP1 regulates migration integral to mitochondrial calcium. As we show in the paper, the close relationship between dynamics of mitochondrial fission and the mitochondrial Ca^{2+} regulation in the pathological process of pulmonary vasculature may provide us combined therapeutic targets of lung disease.

The regulation of mitochodrial Ca^{2+} is closely related with mitochondrial fission and fusion dynamics. Our results prove that DRP1 inhibited intramitochondrial Ca^{2+} concentration under hypoxic condition in the pulmonary endothelial cells (Figure 5A, 5C). More importantly, the MCU specific blocker Ru360 decreased caspase-3 activation, reduced DNA chromatin fragmentation, and downregulated Annexin V-positive cell apoptosis which are all markedly reversed by siDRP1 (Figure 8B-D). This means that mitochondrial Ca^{2+} mediates in the apoptosis inhibited by DRP1, in accordance with the report that mitochondrial Ca^{2+} loading is followed by apoptotic cell death [Orrenius et al., 2003] and controlled by mitochondrial fission in Hela cells [Szabadkai et al., 2004].

We explored the DRP1 regulated mitochondrial Ca^{2+} in PAECs, subsequently leaded to multiple biological effects correlated with hypoxia pulmonary hypertension. Couples of questions still need to be clarified in the future studies. We only find that Mdivi-1 reduced the angiogenesis in chronic hypoxic pulmonary hypertension and it is possible that Mdivi-1 could influence other PAH models. Besides, recent studies focus on the fission protein effect in the proliferation of PASMCs [Marsboom et al., 2012] and in the migration, proliferation, and apoptosis of PAECs by our team. Future research is necessary to elucidate the role of fusion protein in the pathological process and molecular mechanism of PAH.

In this paper, we found that inhibitor of MCU could participate in the mitochondrial fission protein DRP1 mediating in the migration, proliferation, and apoptosis of PAECs, leading to pulmonary angiogenesis. Targeting at the DRP1 signaling system may be a potential strategy for treatment of PAH. Thus, these findings may have important implications for the understanding and treatment of this devastating disease.

ACKNOWLEDGMENT

We thank Dr. Chun Jiang (Georgia State University, Atlanta, USA) for revising the manuscript.

REFERENCES

Birdsey GM,Dryden NH, Shah AV, Hannah R, Hall MD, Haskard DO, Parsons M, Mason JC, Zvelebil M, Gottgens B, Ridley AJ, Randi AM. 2012. The transcription factor Erg regulates expression of histone deacetylase 6 and multiple pathways involved in endothelial cell migration and angiogenesis. Blood 119:894–903.

Brooks C, Wei Q, Cho SG, Dong Z. 2009. Regulation of mitochondrial dynamics in acute kidney injury in cell culture and rodent models. J Clin Invest 119:1275–1285.

Chen Y, Csordas G, Jowdy C, Schneider TG, Csordas N, Wang W, Liu Y, Kohlhaas M, Meiser M, Bergem S, Nerbonne JM, Dorn GW, 2nd, Maack C 2012. Mitofusin 2-containing mitochondrial-reticular microdomains direct rapid cardiomyocyte bioenergetic responses via interorganelle Ca(2+) crosstalk. Circ Res 111:863–875.

Correa F, Soto V, Zazueta C. 2007. Mitochondrial permeability transition relevance for apoptotic triggering in the post-ischemic heart. Int J Biochem Cell Biol 39:787–798.

Courboulin A, Tremblay VL, Barrier M, Meloche J, Jacob MH, Chapolard M, Bisserier M, Paulin R, Lambert C, Provencher S, Bonnet S. 2011. Kruppel-like factor 5 contributes to pulmonary artery smooth muscle proliferation and resistance to apoptosis in human pulmonary arterial hypertension. Respir Res 12:128.

Galie N, Corris PA, Frost A, Girgis RE, Granton J, Jing ZC, Klepetko W, McGoon MD, McLaughlin VV, Preston IR, Rubin LJ, Sandoval J, Seeger W, Keogh A. 2013. Updated treatment algorithm of pulmonary arterial hypertension. J Am Coll Cardiol 62:D60–D72.

Gavrieli Y, Sherman Y, Ben-Sasson SA. 1992. Identification of programmed cell death in situ via specific labeling of nuclear DNA fragmentation. J Cell Biol 119:493–501.

Graupera M, Guillermet-Guibert J, Foukas LC, Phng LK, Cain RJ, Salpekar A, Pearce W, Meek S, Millan J, Cutillas PR, Smith AJ, Ridley AJ, Ruhrberg C, Gerhardt H, Vanhaesebroeck B. 2008. Angiogenesis selectively requires the p110alpha isoform of PI3K to control endothelial cell migration. Nature 453:662–666.

Hajnoczky G, Robb-Gaspers LD, Seitz MB, Thomas AP. 1995. Decoding of cytosolic calcium oscillations in the mitochondria. Cell 82:415–424.

Howell K, Preston RJ, McLoughlin P. 2003. Chronic hypoxia causes angiogenesis in addition to remodelling in the adult rat pulmonary circulation. J Physiol 547:133–145.

Jones EA, le Noble F, Eichmann A. 2006. What determines blood vessel structure? Genetic prespecification vs. hemodynamics. Physiology (Bethesda) 21:388–395.

Kannurpatti SS, Biswal BB. 2008. Mitochondrial Ca2+ uniporter blockers influence activation-induced CBF response in the rat somatosensory cortex. J Cereb Blood Flow Metab 28:772–785.

Lee S, Park YY, Kim SH, Nguyen OT, Yoo YS, Chan GK, Sun X, Cho H. 2014. Human mitochondrial Fis1 links to cell cycle regulators at G2/M transition. Cell Mol Life Sci 71:711–725.

Legha RK, Novins D. 2012. The role of culture in substance abuse treatment programs for American Indian and Alaska Native communities. Psychiatr Serv 63:686–692.

Ma J, Liang S, Wang Z, Zhang L, Jiang J, Zheng J, Yu L, Zheng X, Wang R, Zhu D. 2010. ROCK pathway participates in the processes that 15-hydroxyeicosatetraenoic acid (15-HETE) mediated the pulmonary vascular remodeling induced by hypoxia in rat. J Cell Physiol 222:82–94.

Ma C, Li Y, Ma J, Liu Y, Li Q, Niu S, Shen Z, Zhang L, Pan Z, Zhu D. 2011. Key role of 15-lipoxygenase/15-hydroxyeicosatetraenoic acid in pulmonary vascular remodeling and vascular angiogenesis associated with hypoxic pulmonary hypertension. Hypertension 58:679–688.

Ma J, Zhang L, Han W, Shen T, Ma C, Liu Y, Nie X, Liu M, Ran Y, Zhu D. 2012. Activation of JNK/c-Jun is required for the proliferation, survival, and angiogenesis induced by EET in pulmonary artery endothelial cells. J Lipid Res 53:1093–1105.

Ma C, Wang Y, Shen T, Zhang C, Ma J, Zhang L, Liu F, Zhu D. 2013. Placenta growth factor mediates angiogenesis in hypoxic pulmonary hypertension. Prostaglandins Leukot Essent Fatty Acids 89:159–168.

Marsboom G, Toth PT, Ryan JJ, Hong Z, Wu X, Fang YH, Thenappan T, Piao L, Zhang HJ, Pogoriler J, Chen Y, Morrow E, Weir EK, Rehman J, Archer SL. 2012. Dynamin-related protein 1-mediated mitochondrial mitotic fission permits hyperproliferation of vascular smooth muscle cells and offers a novel therapeutic target in pulmonary hypertension. Circ Res 110:1484–1497.

Orrenius S, Zhivotovsky B, Nicotera P. 2003. Regulation of cell death: the calcium-apoptosis link. Nat Rev Mol Cell Biol 4:552–565.

Otsuga D, Keegan BR, Brisch E, Thatcher JW, Hermann GJ, Bleazard W, Shaw JM. 1998. The dynamin-related GTPase, Dnm1p, controls mitochondrial morphology in yeast. J Cell Biol 143:333–349.

Pak O, Aldashev A, Welsh D, Peacock A. 2007. The effects of hypoxia on the cells of the pulmonary vasculature. Eur Respir J 30:364–372.

Parra V, Eisner V, Chiong M, Criollo A, Moraga F, Garcia A, Hartel S, Jaimovich E, Zorzano A, Hidalgo C, Lavandero S. 2008. Changes in mitochondrial dynamics during ceramide-induced cardiomyocyte early apoptosis. Cardiovasc Res 77:387–397.

Paterlini P, Suberville AM, Zindy F, Melle J, Sonnier M, Marie JP, Dreyfus F, Brechot C. 1993. Cyclin A expression in human hematological malignancies: a new marker of cell proliferation. Cancer Res 53:235–238.

Pivovarova NB, Andrews SB. 2010. Calcium-dependent mitochondrial function and dysfunction in neurons. FEBS J 277:3622–3636.

Shen T, Ma J, Zhang L, Yu X, Liu M, Hou Y, Wang Y, Ma C, Li S, Zhu D. 2013. Positive feedback-loop of telomerase reverse transcriptase and 15-lipoxygenase-2 promotes pulmonary hypertension. PLoS One 8:e83132.

Suen DF, Norris KL, Youle RJ. 2008. Mitochondrial dynamics and apoptosis. Genes Dev 22:1577–1590.

Szabadkai G, Simoni AM, Chami M, Wieckowski MR, Youle RJ, Rizzuto R. 2004. Drp-1-dependent division of the mitochondrial network blocks intraorganellar Ca2+ waves and protects against Ca2+-mediated apoptosis. Mol Cell 16:59–68.

Wan YY, Zhang JF, Yang ZJ, Jiang LP, Wei YF, Lai QN, Wang JB, Xin HB, Han XJ. 2014. Involvement of Drp1 in hypoxia-induced migration of human glioblastoma U251 cells. Oncol Rep 32:619–626.

Westermann B. 2010. Mitochondrial fusion and fission in cell life and death. Nat Rev Mol Cell Biol 11:872–884.

White K, Dempsie Y, Caruso P, Wallace E, McDonald RA, Stevens H, Hatley ME, Van Rooij E, Morrell NW, MacLean MR, Baker AH. 2014. Endothelial apoptosis in pulmonary hypertension is controlled by a microRNA/programmed cell death 4/caspase-3 axis. Hypertension 64:185–194.

Yang SY, Kim NH, Cho YS, Lee H, Kwon HJ. 2014. Convallatoxin, a dual inducer of autophagy and apoptosis, inhibits angiogenesis in vitro and in vivo. PLoS One 9:e91094.

Zhao J, Zhang J, Yu M, Xie Y, Huang Y, Wolff DW, Abel PW, Tu Y. 2013. Mitochondrial dynamics regulates migration and invasion of breast cancer cells. Oncogene 32:4814–4824.

Zhu D, Medhora M, Campbell WB, Spitzbarth N, Baker JE, Jacobs ER. 2003. Chronic hypoxia activates lung 15-lipoxygenase, which catalyzes production of 15-HETE and enhances constriction in neonatal rabbit pulmonary arteries. Circ Res 92:992–1000.

Ziviani E, Tao RN, Whitworth AJ. 2010. Drosophila parkin requires PINK1 for mitochondrial translocation and ubiquitinates mitofusin. Proc Natl Acad Sci U S A 107:5018–5023.